

**NEUTRON INDUCED  $^{55}\text{Mn}$  REACTION IN THE ENERGY RANGE 0.001MeV TO 40MeV**

A. K. M. Rezaur Rahman<sup>1a\*</sup>, Taslim Hoque Happy<sup>2a</sup>, Mustofa Khalid Ovi<sup>3a</sup>, Abdul Awal<sup>4b</sup>, Mark Anthony Bromuela<sup>5a</sup>, MD. Jubayer Rahman Akhand<sup>6c</sup>, Shyamal Ranjan Chakraborty<sup>7a</sup>, and A. K. M. Moinul Haque Meaze<sup>8a</sup>

**Abstract:** Neutron induced  $^{55}\text{Mn}$  reactions were evaluated in the energy range 0.001 MeV to 40 MeV using TALYS 1.95 computer code. During this evaluation, local and global parameterisations of Koning and Delaroche were used in nuclear optical model. Comparisons were made with experimental data, collected from EXFOR and other sources. Some optical model parameters (OMP) were needed to be adjusted for better agreement between theoretical calculations and experimental findings. Various evaluated libraries such as ENDF, JENDL etc. were checked and compared with our evaluation. TALYS evaluation showed better agreement when parameters were adjusted.

**Keywords:** Neutron cross section, manganese, optical model, TALYS, nuclear data evaluation

**1. Introduction**

Application of developed nuclear science that has and will have an important impact on society – nuclear energy, medicine, security, material characterisation, geological exploration, radiation safety and protection and the promise of fusion energy (Plompen et al. 2020). Accurate nuclear cross section data that need to be provided to predict the tritium breeding capability, assess the shielding efficiency, estimate the nuclear power generated in the system, and produce activation and radiation damaged data for the irradiated materials/components (Fischer et al. 2018). The new evaluated nuclear data plays an efficient role in nuclear technology (Rahman & Awal 2020; Rahman et al. 2019; Lorenz & Schmidt, 1986). Evaluation of nuclear data is a continuous process and the evaluation of cross-section data is very important for those who have experimental difficulty and are hopeless for measuring the cross-section data (Rahman & Zubair 2020a; Rahman 2012a). So, the cross-section evaluation for materials has special importance in systematic use of neutron induced reaction cross-section. (Rahman 2012b). In nuclear data evaluations, theoretical calculation is essential and the evaluated data from the theoretical calculation plays an important role on their applications to fusion reactor neutronics. Precise data on cross sections are needed for comprehensive computer modeling for future experiments. Success of many nuclear research

programs depends on the quality of nuclear database (Rahman & Zubair 2020b; Reshid 2013; Shibata 1989).

Manganese is a very hard, brittle, grey-white transitional metal that has only one stable isotope  $^{55}\text{Mn}$  with 100% abundance. It is a nutritional inorganic trace element required for a variety of physiological processes including development, antioxidant defenses, reproduction and neuronal function (Horning et al. 2015; Kwakye 2015). It is a key component of aluminium copper alloys which is widely used in accelerator technology, fission and fusion devices as structural materials, dosimeter materials, control module etc. Manganese is also essential for anti-tumor immune responses (Lv et al. 2020). At present, 85% to 90% stainless steel contains around 2% of manganese. Many radioactive isotopes are produced from  $n+^{55}\text{Mn}$  reactions like  $^{54}\text{Mn}$ ,  $^{56}\text{Mn}$ ,  $^{55}\text{Mn}$ ,  $^{51}\text{Cr}$ . Cancer can be obstructed by summing some manganese supplements in daily diet. Manganese has also displayed ability in controlling the balance of sugar in human blood by normalizing insulin synthesis and secretion and can prevent diabetes (Kaziet al. 2008). Al-Mn alloys are possibly the most important of the non-age hardenable alloys of aluminium and generally contain between 0.25 to 1.25% Mn (Zamin 1981). Cu–Al–Mn alloys are well-known types of shape memory alloys introduced to technological use (Canbay et al. 2014).

Accurate neutron capture cross-sections of  $^{55}\text{Mn}$  are important for reactor design in view of its use as an alloy structural material. Cross-section data provide important information of various kinds of actions and these data can be used for different types of researches. Data evaluation of  $^{55}\text{Mn}$  is very essential for the design of nuclear device and many features are

**Authors information:**

<sup>a</sup>Department of Physics, University of Chittagong, Chittagong, BANGLADESH.

E-mail: rezaur.physics@cu.ac.bd<sup>1</sup>;  
taslimhoque529@gmail.com<sup>2</sup>;  
mustafakhalid.soaf@gmail.com<sup>3</sup>;  
mabromuela.88@gmail.com<sup>5</sup>; shyamal@cu.ac.bd<sup>7</sup>;  
meaze@cu.ac.bd<sup>8</sup>

<sup>b</sup>Obninsk Institute for Nuclear Power Engineering of MEPhI, RUSSIA. E-mail: abdulawal1993@gmail.com<sup>4</sup>

<sup>c</sup>Bangladesh Military Academy, Chittagong, BANGLADESH. E-mail: jubayer27@gmail.com<sup>6</sup>

\*Corresponding Author: rezaur.physics@cu.ac.bd

**Received:** December 10, 2021

**Accepted:** July 17, 2022

**Published:** October 31, 2023

currently placed on it for using fusion reactor neutronics (Shibata 1989).  $^{55}\text{Mn}$  is used as an alloy of structural material in which accurate capture cross-section is necessary for the future of reactors. Reliable estimation of the activation levels of manganese is needed to support critical safety analyses (Barough et al. 2017). In nuclear data evaluations, theoretical calculation is essential and the evaluated data from the theoretical calculation play an important role on their applications to fusion reactor neutronics.

Experimental nuclear data are stored in the EXFOR database. Collection of nuclear data from nuclear models is subject to uncertainties, coming from the imperfect knowledge of model parameters or the models themselves. These two sources need to be combined. An isotopic evaluation results in a probability distribution for the observables of a (usually) neutron induced reaction on that isotope. The most probable solution is the evaluation of nuclear data, while the full probability distribution is often missing. Nevertheless, this is often the case for many of the world libraries, the evaluated file is the evaluators' "best shot" (Koning 2015).

In our current research, we aim to analyze the nature of nuclear reaction for  $n+^{55}\text{Mn}$  in the energy range 0.001MeV to 40 MeV. The experimental values from EXFOR data file of INDC of IAEA and evaluated values from various data libraries are to be used for evaluation purpose. Reaction channels and production routes are also analyzed. Discrepancies will be mitigated by adjusting the parameters of necessary nuclear model(s).

## 2. Theoretical Model and Evaluation Tool

TALYS is the modern nuclear data evaluation code system (Koning 2015). It is a software for the simulation of nuclear reactions and a versatile tool to analyze basic microscopic experiments. This code is used to generate nuclear data for all open channels in the fast neutron energy region, that is, beyond the resonance region. In situations where experimental data are unavailable, TALYS is used for the prediction and extrapolation of data (Koning & Rochman, 2012). The objective of TALYS is to provide a complete simulation of nuclear reactions in the 1 KeV-200MeV energy range, through an optimal combination of reliable nuclear models, flexibility and user-friendliness.

Optical model returns a prediction for the basic observable, namely the elastic angular distribution as well as polarization, the reaction and total cross section and for low energies, the  $s$ ,  $p$ -wave strength functions and the potential scattering radius  $R'$ . When enough experimental scattering data of a certain nucleus are available, a so called local OMP can be constructed. TALYS retrieves all the parameters  $v_1$ ,  $v_2$ , etc. of these local OMP automatically from the nuclear structure and model parameter database. The global neutron OMP, validated for  $0.001 \leq E \leq 200\text{MeV}$  and  $24 \leq A \leq 209$ .

Pre-equilibrium emission takes place after the first stage of the reaction but long before statistical equilibrium of the compound nucleus is attained. It is imagined that the incident particle step-by-step creates more complex states in the compound system and gradually loses its memory of the initial energy and direction. Pre-equilibrium processes cover a sizable part of the reaction cross section for incident energies between 10 and (at least) 200MeV. Pre-equilibrium reactions have been modeled both classically and quantum-mechanically and both are included in TALYS.

Various models for direct reactions are included in the program: DWBA for spherical nuclides, coupled-channels for deformed nuclides, the weak-coupling model for odd nuclei, and also a giant resonance contribution to the continuum. In all cases, TALYS drives the ECIS-06 code to perform the calculations. The results are presented as discrete state cross sections and angular distributions, or as contributions to the continuum.

During this calculation, local and global parameterisations of Koning and Delaroche were used (Koning & Delaroche 2003). The parameter set are given below, where, the units are in fm:

$$r_v = 1.3039 - 0.4054 A^{-1/3} \quad (1)$$

$$a_v = 0.6778 - 1.487 \times 10^{-4} A \quad (2)$$

$$r_D = 1.3424 - 0.01585 A^{1/3} \quad (3)$$

$$a_D = 0.5446 - 1.656 \times 10^{-4} A \quad (4)$$

$$r_{SO} = 1.1854 - 0.647 A^{-1/3} \quad (5)$$

$$a_{SO} = 0.59 \quad (6)$$

### 3. Results and Discussions

Based on our evaluation, the reaction grid for  $n + {}^{55}\text{Mn}$  is shown in Fig. 1. Different reaction channels, residual production and production routes of residual production are tabulated in Table 1.

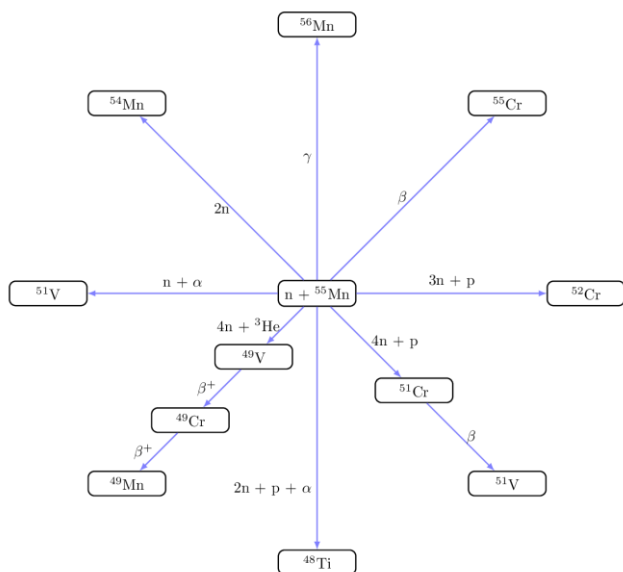


Figure 1. Main reaction grid for  $n + {}^{55}\text{Mn}$  reaction.

Table 1. Table for residue particle product, reaction channels, and most probable routes according to this work.

Sl. No.	Reaction Channel	Half-life of Residue Particle	Residue Particle Production Routes	Most Probable Route
1	${}^{55}\text{Mn} (n, g)$ ${}^{56}\text{Mn}$	2.5789 hr	(n, g)	(n, g)
2	${}^{55}\text{Mn} (n, \text{inl})$ ${}^{55}\text{Mn}$	Stable	(n, inl)	(n, inl)
3	${}^{55}\text{Mn} (n, 2n)$ ${}^{54}\text{Mn}$	312.12 d	(n, 2n)	(n, 2n)
4	${}^{55}\text{Mn} (n, p)$ ${}^{55}\text{Cr}$	3.4967 min	(n, p)	(n, p)
5	${}^{55}\text{Mn} (n, d)$ ${}^{54}\text{Cr}$	Stable	(n, d) (n, np)	(n, np)
6	${}^{55}\text{Mn} (n, t)$ ${}^{53}\text{Cr}$	Stable	(n, t) (n, nd) (n, 2np)	(n, 2np)
7	${}^{55}\text{Mn} (n, 3\text{He})$ ${}^{53}\text{V}$	1.6 min	(n, he3) (n, pd) (n, n2p)	(n, n2p)
8	${}^{55}\text{Mn} (n, \alpha)$ ${}^{52}\text{V}$	3.7433 min	(n, $\alpha$ )	(n, $\alpha$ )

In the grid, only main reactions are considered. There are lots of isotopes of manganese, among them only  ${}^{55}\text{Mn}$  is the stable isotope with 100% abundance and the others are radioisotopes, like:  ${}^{46}\text{Mn}$ ,  ${}^{47}\text{Mn}$ ,  ${}^{48}\text{Mn}$ ,  ${}^{49}\text{Mn}$ ,  ${}^{50}\text{Mn}$ ,  ${}^{51}\text{Mn}$ ,  ${}^{52}\text{Mn}$ ,  ${}^{54}\text{Mn}$ ,  ${}^{56}\text{Mn}$ ,  ${}^{57}\text{Mn}$ . These radioactive isotopes emit  $\beta$  ( $\beta^+$ ,  $\beta^-$ ) particles with the half-life of 36.2ms to 312.12 days. From  $n + {}^{55}\text{Mn}$  reaction many isotopes are produced, the most significant isotopes we considered here,  ${}^{54}\text{Mn}$ ,  ${}^{56}\text{Mn}$ ,  ${}^{55}\text{Mn}$ ,  ${}^{51}\text{Cr}$ ,  ${}^{52}\text{Cr}$ ,  ${}^{49}\text{V}$ ,  ${}^{51}\text{V}$ , and  ${}^{48}\text{Ti}$ .

All sorts of reaction processes happened in  $n + {}^{55}\text{Mn}$  reaction are shown in Fig. 2. It is seen that the cross-section data of non-elastic, elastic, shape-elastic and reaction cross-section value are quite closer to the total cross-section data; with some fluctuation, they have significant cross-section data in both low and high energies.

The cross-section value of compound non-elastic cross-section for  $n + {}^{55}\text{Mn}$  is too low at the higher energy range. It has been seen that, between the energy ranges 1 MeV to 10 MeV, cross-section values of compound non-elastic cross-section are increasing slowly to the higher energy range, but it is damping about the energy range 15 MeV (about 900 mb). The cross-section values of the compound elastic cross-section for  $n + {}^{55}\text{Mn}$  are reduced to zero in the energy range between 10 MeV to 15 MeV, while its lower energy range contains momentous cross-section data. Direct reaction process starts after 0.2 MeV and reaches maxima around 2 MeV (about 116 mb). Then it reduces slowly. Pre-equilibrium reaction begins at 3 MeV. For Pre-equilibrium, cross section rises rapidly, immediately after the straight point. Pre-equilibrium process rapidly ascends toward its flat maxima (about 700 mb) around 30 MeV.

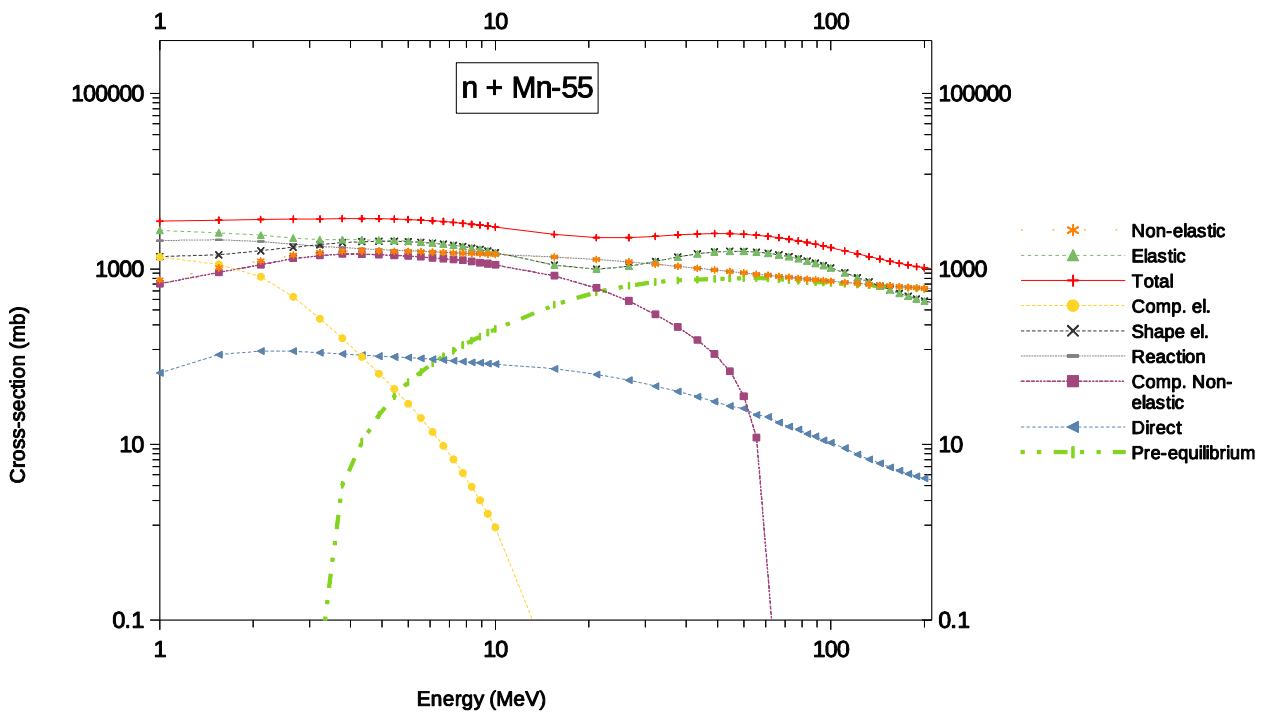


Figure 2. Various scattering and reaction cross-section from n + <sup>55</sup>Mn reaction.

The default model used by TALYS is the two-component exciton model with collision probabilities based on the effective squared matrix element. To fit experimental data, the model parameters can be adjusted via adjustable parameters through different keywords. The *rvadjust* is a multiplier to adjust the OMP parameter  $r_v$  which has default value 1.0 for all nuclei. We changed its value to 1.0502 for <sup>55</sup>Mn for better agreement with experimental values. Multiplier to adjust the OMP parameter  $a_v$  is *avadjust* which has default value 1.0. We have changed its value 0.8199 for better agreement with experimental values. These changes are tabulated in Table 2.

Table 2. Table for showing OMP values

Calculation Type	<i>Rvadjust</i>	<i>Avadjust</i>
Default	1.0	1.0
Adjusted	1.0502	0.8199

For adjusting our parameters to the desired values above, multiple reruns on TALYS were made with new and better values as to fit with the experimental plots. The values were chosen as prescribed by Eqns. (1-2). All other parameter values were kept default in TALYS. The values were given up to four decimal figures for accuracy which we deemed fitting sufficiently such experimental plots.

### 3.1 Total Scattering Cross-Section

From Fig. 3, we compared our calculated values of total scattering cross-section for  $n+^{55}\text{Mn}$  reaction with the experimental and evaluated values which were collected from EXFOR and ENDF. Fig. 3 shows that both the experimental and evaluated data show several fluctuations in structure below 0.1 MeV. From this present work we can observe that after 2MeV, our calculated values of total Scattering cross-section have a good agreement to the cross-section data of different sources and we can also see that there is much resonance at lower energy range region. Calculated data with default parameters do not match

with experimental values at 0.01MeV. At 0.01MeV, the total scattering cross section is up to 25000 mb (Cote et al 1964). According to calculated values with default parameters, the total scattering cross section is around 30000mb. So, adjustment is made. After adjustment, our calculated values pass through the experimental data at 0.01 MeV – 0.3MeV region. But, the fluctuation in this region could not be well produced. There is no experimental and evaluated cross-section values from 0.3MeV to 2MeV as far as we have searched.

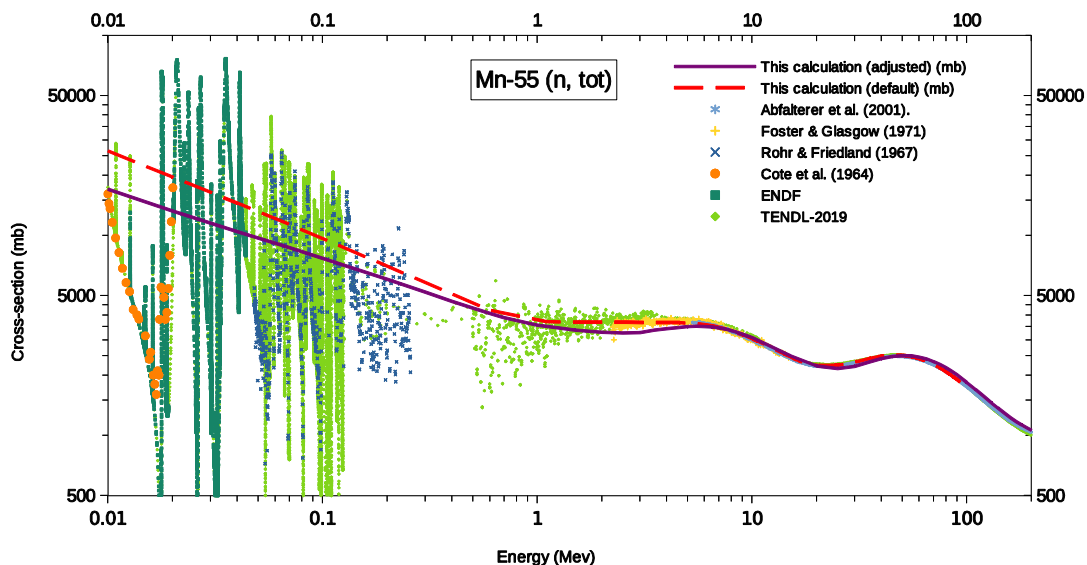


**Figure 3.** The comparison graph between experimental data, evaluated data and calculated values of total cross-section for  $n + ^{55}\text{Mn}$  reaction.

### 3.2 Neutron Elastic Scattering Cross-Section

Neutron elastic scattering cross sections for  $^{55}\text{Mn}$  are calculated from 0.01MeV, and comparison is made between the experimental and evaluated data. Fig. 4 shows the comparison with experimental values and with evaluated values from ENDF. At very low neutron energy (0.01 MeV) our calculated data with default parameters do not match with experimental values. So we adjusted parameters. At 0.1 MeV, the elastic cross section is more than 6000 mb. But its values decline rapidly with energy. At low energy region (0.2 MeV-0.6MeV) calculation with default parameters shows a little bit higher cross sections. The calculation

with parameter adjustment makes the agreement better with experimental values in that region. The pattern of the experimental and theoretical curves agrees with each other and the calculated value passes through the evaluated and experimental data at 1MeV-100MeV region. From this present work, it has been noticed that there are high resonances in the lower energy range and our calculated values have quite good similarity to the experimental values at the higher energy range and pass through the resonance region.

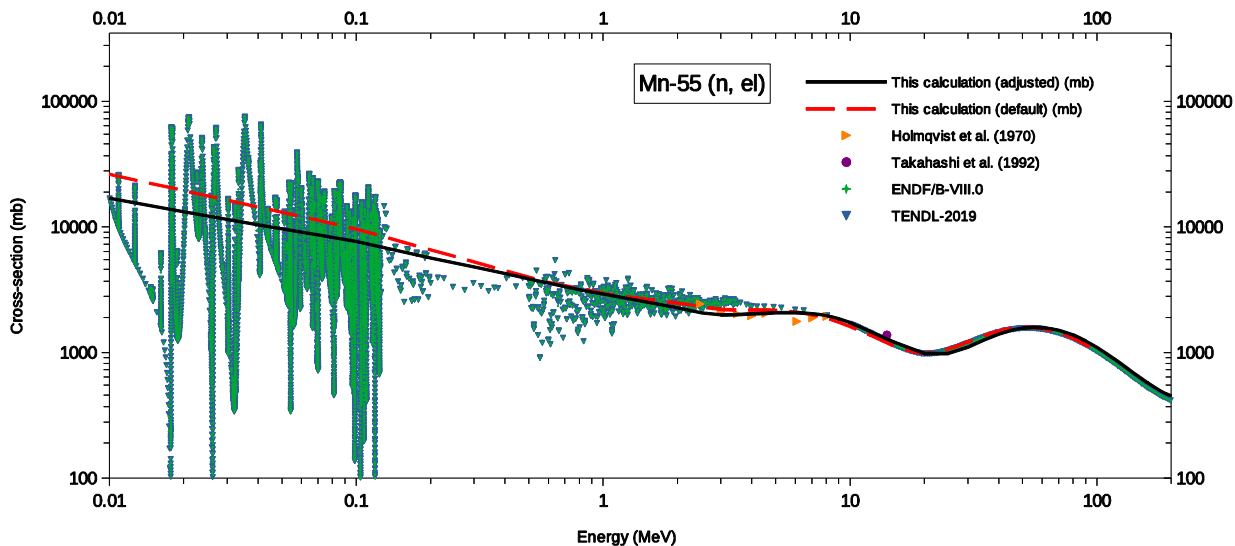
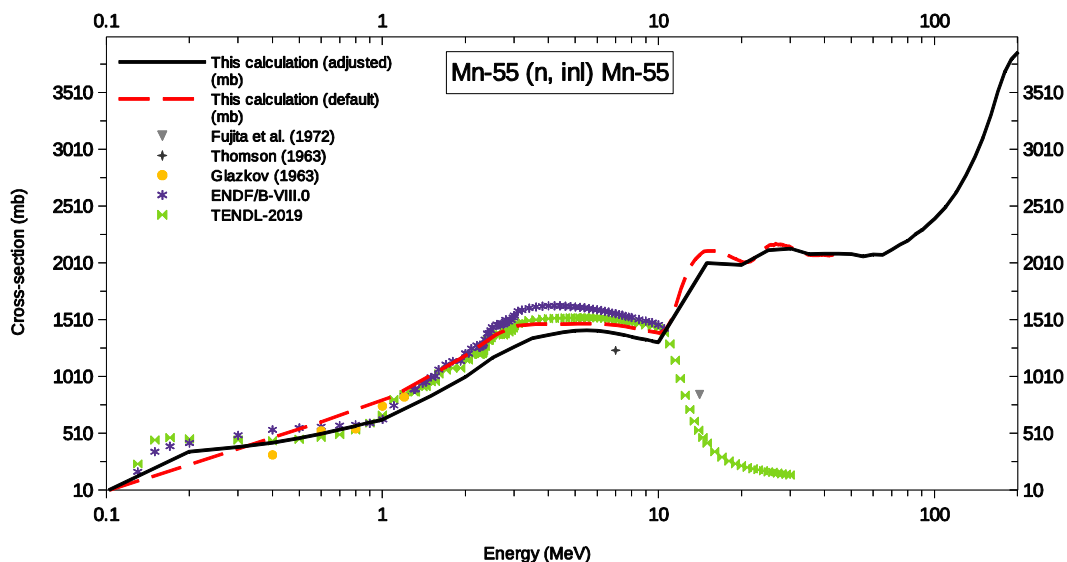


Figure 4. The elastic scattering cross-section for  $n + ^{55}\text{Mn}$  reaction.

### 3.3 Total Neutron Production Cross-Section

From Fig. 5, we have compared our present work for calculated total neutron production of  $n+^{55}\text{Mn}$  reaction with the experimental and evaluated values which are collected from different sources. In the energy region 0.1MeV-1 MeV calculated data with default parameters do not match with evaluated and experimental values. But the calculated curve with adjusted parameters passes through the evaluated and experimental data. From this present work it has been observed that the experimental and evaluated values of total neutron production

cross-section have good agreement with our calculated values with adjusted parameters at lower energy range, except the experimental values of Fujita et al. (1972) and Thomson (1963). There is no experimental and evaluated values at higher energy range as far as we searched. At 10MeV, the total neutron production cross-section is more than 1250 mb. At 10MeV – 20 MeV, its value inclines with energy. There is a flat valley in the curve at 50MeV-100MeV region according to our calculated values.



**Figure 5.** The comparison graph between experimental data, evaluated data and calculated data value of total neutron production cross-section for  $n + ^{55}\text{Mn}$  reaction.

### 3.4 Total Proton Production Cross-Section

From Fig. 6, we compared our calculated values of total proton production for  $n + {}^{55}\text{Mn}$  reaction with the experimental and evaluated values which are collected from different experimental and evaluated sources. From this present work, it has been seen that our calculated values are almost similar to the experimental and evaluated values. We did not find any cross-

section value at higher energy range as far as we searched as well as at the lower energy range, most of the experimental values were found between 6 MeV to 15 MeV. We can see that at the lower energy range our calculated values have good agreement with evaluated and experimental values we collected for the total proton production for  $n + {}^{55}\text{Mn}$  reaction.

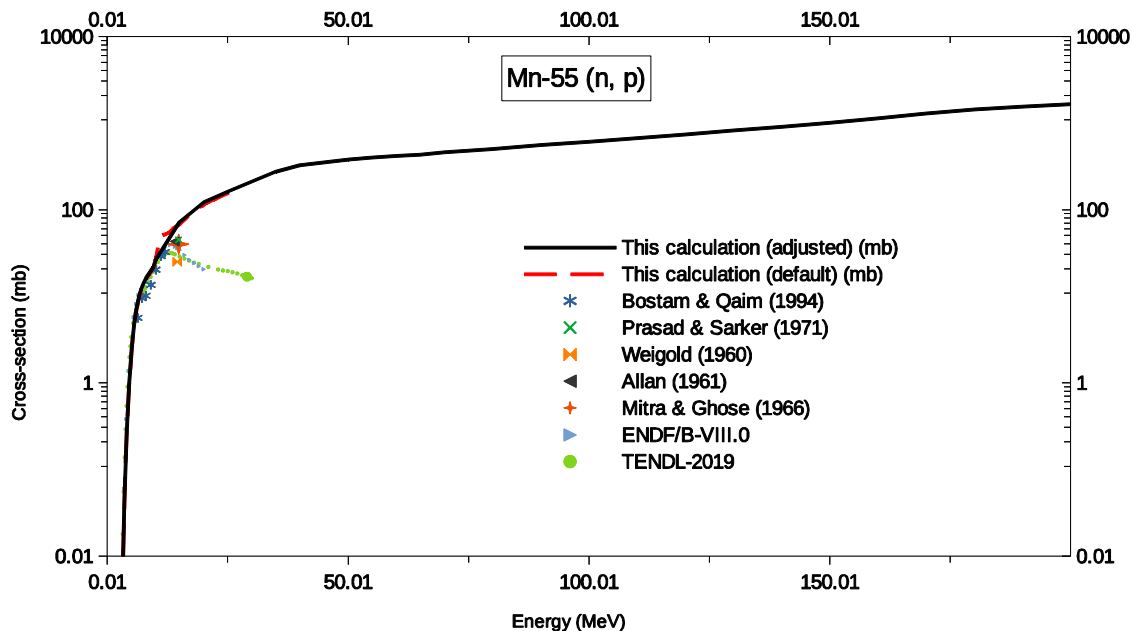


Figure 6. Comparison graph of total proton production from  $n+{}^{55}\text{Mn}$  reaction.

By adjusting the parameters, we have increased the value of the real potential ( $r_v$ ) and decreased the diffuseness parameter ( $a_v$ ) for probability of interaction decrease. As a result, the excitation function with adjusted parameters comes closer to the experimental values.

## 4. Conclusion

We know, cross-section data of  ${}^{55}\text{Mn}$  are used for reactor or nuclear device designing, safety analysis or different types of research. We compared our evaluated cross-section values with different experimental and evaluated data values from different sources. The present evaluation with default parameters agrees well with evaluated and experimental data except for 0.01 – 10 MeV region. For better agreement, hence, geometrical and diffuseness parameters of optical model are adjusted so that more accurate data can be used for application if experimental data are unavailable.

Our evaluation shows that among all scattering and reaction cross-sections for  $n+{}^{55}\text{Mn}$  reaction, the cross-section data of non-elastic, elastic-scattering, shape-elastic scattering and reaction cross-section are nearly equal to the total cross-section data values with some fluctuation and they have effective cross-section data in both low and high energy ranges too. Our calculated total and elastic cross section values with adjusted

parameters agree well with experimental values in the overall investigated energy range. Experimental and evaluated cross-section data at lower energy range have good agreement with our calculated cross-section data with adjusted parameters of total neutron production for  $n+{}^{55}\text{Mn}$ . At the lower energy range, our calculated values of total proton production data with adjusted parameters for  $n+{}^{55}\text{Mn}$  reaction are also in good agreement with evaluated and experimental cross-section values.

## 6. References

- Abfalterer, W. P., Bateman, F. B., Dietrich, F. S., Finlay, R. W., Haight, R. C., & Morgan, G. L. (2001). Measurement of neutron total cross sections up to 560 MeV. *Physical Review C*, 63(4), 44608. <https://doi.org/10.1103/PhysRevC.63.044608>
- Allan, D. L. (1961). An experimental test of the statistical theory of nuclear reactions. *Nuclear Physics*, 24, 274–299. [https://doi.org/10.1016/0029-5582\(61\)90380-7](https://doi.org/10.1016/0029-5582(61)90380-7)
- Barough, M. S., Bharud, V. D., Patil, B. J., Attar, F. M. D., Bhoraskar, V. N., & Dhole, S. D. (2017). Measurement and Estimation of Cross Sections for  ${}^{55}\text{Mn}(n, \gamma){}^{56}\text{Mn}$  and  ${}^{65}\text{Cu}(n, \gamma){}^{66}\text{Cu}$  Reactions Using Accelerator-Based Neutron Source. *Nuclear Science and Engineering*,

- 187(3), 302–311.  
<https://doi.org/10.1080/00295639.2017.1323505>
- Bostan, M., & Qaim, S. M. (1994). Excitation functions of threshold reactions on  $^{45}\text{Sc}$  and  $^{55}\text{Mn}$  induced by 6 to 13 MeV neutrons. *Physical Review C*, *49*(1), 266–271.  
<https://doi.org/10.1103/PhysRevC.49.266>
- Canbay, C. A., Ozgen, S., & Genc, Z. K. (2014). Thermal and microstructural investigation of Cu–Al–Mn–Mg shape memory alloys. *Applied Physics A*, *117*(2), 767–771.  
<https://doi.org/10.1007/s00339-014-8643-5>
- Coté, R. E., Bollinger, L. M., & Thomas, G. E. (1964). Total Neutron Cross Section of Manganese. *Physical Review*, *134*(5B), B1047–B1051.  
<https://doi.org/10.1103/PhysRev.134.B1047>
- Fischer, U., Angelone, M., Avrigeanu, M., Avrigeanu, V., Bachmann, C., Dzysiuk, N., Fleming, M., Konobeev, A., Kodeli, I., Koning, A., Leeb, H., Leichtle, D., Ogando, F., Pereslavtsev, P., Rochman, D., Sauvan, P., & Simakov, S. (2018). The role of nuclear data for fusion nuclear technology. *Fusion Engineering and Design*, *136*.  
<https://doi.org/10.1016/j.fusengdes.2018.01.036>
- Foster, D. G., & Glasgow, D. W. (1971). Neutron Total Cross Sections, 2.5–15 MeV. I. Experimental. *Physical Review C*, *3*(2), 576–603. <https://doi.org/10.1103/PhysRevC.3.576>
- Fujita, I., Sonoda, M., Katase, A., Wakuta, Y., Tawara, H., Hyakutake, M., & Iwatani, K. (1972). Inelastic Scattering of 14MeV Neutrons by Medium Weight Nuclei. *Journal of Nuclear Science and Technology*, *9*(5), 301–309.  
<https://doi.org/10.1080/18811248.1972.9734846>
- Glazkov, N. P. (1963). Cross sections of the inelastic scattering of neutrons with energies of 0.4–1.2 MeV on medium and light nuclei. *Soviet Atomic Energy*, *15*(5), 1173–1176. <https://doi.org/10.1007/BF01115942>
- Holmqvist, B., Wiedling, T., Benzi, V., & Zuffi, L. (1970). Analysis of fast neutron elastic scattering from tantalum using a non-spherical optical potential. *Nuclear Physics A*, *150*(1), 105–113.  
[https://doi.org/https://doi.org/10.1016/0375-9474\(70\)90460-4](https://doi.org/https://doi.org/10.1016/0375-9474(70)90460-4)
- Horning, K. J., Caito, S. W., Tipps, K. G., Bowman, A. B., & Aschner, M. (2015). Manganese Is Essential for Neuronal Health. *Annual review of nutrition*, *35*, 71–108. <https://doi.org/10.1146/annurev-nutr-071714-034419>
- Kazi, T. G., Afridi, H. I., Kazi, N., Jamali, M. K., Arain, M. B., Jalbani, N., & Kandhro, G. A. (2008). Copper, chromium, manganese, iron, nickel, and zinc levels in biological samples of diabetes mellitus patients. *Biological trace element research*, *122*(1), 1–18.  
<https://doi.org/10.1007/s12011-007-8062-y>
- Koning, A. J. (2015). Bayesian Monte Carlo method for nuclear data evaluation. *The European Physical Journal A*, *51*(12), 184.  
<https://doi.org/10.1140/epja/i2015-15184-x>
- Koning, A. J., & Delaroche, J. P. (2003). Local and global nucleon optical models from 1 keV to 200 MeV. *Nuclear Physics A*, *713*(3), 231–310.  
[https://doi.org/https://doi.org/10.1016/S0375-9474\(02\)01321-0](https://doi.org/https://doi.org/10.1016/S0375-9474(02)01321-0)
- Koning, A. J., & Rochman, D. (2012). Modern Nuclear Data Evaluation with the TALYS Code System. *Nuclear Data Sheets*, *113*(12), 2841–2934.  
<https://doi.org/https://doi.org/10.1016/j.nds.2012.11.002>
- Kwakye, G. F., Paoliello, M. M., Mukhopadhyay, S., Bowman, A. B., & Aschner, M. (2015). Manganese-Induced Parkinsonism and Parkinson's Disease: Shared and Distinguishable Features. *International journal of environmental research and public health*, *12*(7), 7519–7540. <https://doi.org/10.3390/ijerph120707519>
- Lorenz, A., & Schmidt, J. J. (1986). Nuclear data: Serving basic needs of science and technology. *IAEA Bulletin*, *28*(4)17-20.  
<https://www.iaea.org/sites/default/files/28405081720.pdf>
- Lv, M., Chen, M., Zhang, R., Zhang, W., Wang, C., Zhang, Y., Wei, X., Guan, Y., Liu, J., Feng, K., Jing, M., Wang, X., Liu, Y.-C., Mei, Q., Han, W., & Jiang, Z. (2020). Manganese is critical for antitumor immune responses via cGAS-STING and improves the efficacy of clinical immunotherapy. *Cell Research*, *30*(11), 966–979. <https://doi.org/10.1038/s41422-020-00395-4>
- Mitra, B., & Ghose, A. M. (1966). (n, p) cross sections of some low Z nuclei for 14.8 MeV neutrons. *Nuclear Physics*, *83*(1), 157–165.  
[https://doi.org/https://doi.org/10.1016/0029-5582\(66\)90346-4](https://doi.org/https://doi.org/10.1016/0029-5582(66)90346-4)
- Plompen, A. J. M., Cabellos, O., De Saint Jean, C., Fleming, M., Algora, A., Angelone, M., Archier, P., Bauge, E., Bersillon, O., Blokhin, A., Cantargi, F., Chebboubi, A., Diez, C., Duarte, H., Dupont, E., Dyrda, J., Erasmus, B.,

- Fiorito, L., Fischer, U., ... Žerovnik, G. (2020). The joint evaluated fission and fusion nuclear data library, JEFF-3.3. *European Physical Journal A*, 56(7). <https://doi.org/10.1140/epja/s10050-020-00141-9>
- Prasad, R., & Sarkar, D. C. (1971). Measured (n, p) reaction cross-sections and their predicted values at 14.8 MeV. *Il Nuovo Cimento A (1965-1970)*, 3(4), 467–478. <https://doi.org/10.1007/BF02823319>
- Rahman, A. K. M. R. (2012a). Neutron cross-sections for <sup>55</sup>Mn in the energy range from 0.2 to 22 MeV. *Turkish Journal of Physics*. <https://doi.org/10.3906/fiz-1107-3>
- Rahman, A. K. M. R. (2012b). Neutron interaction cross-sections for <sup>27</sup>Al in the energy range from 0.2 to 22 MeV using optical model program. *Science Journal Ubon Ratchathni University, Thailand*, 2.
- Rahman, A. K. M. R., & Awal, A. (2020). Production of <sup>149</sup>Tb, <sup>152</sup>Tb, <sup>155</sup>Tb and <sup>161</sup>Tb from gadolinium using different light-particle beams. *Journal of Radioanalytical and Nuclear Chemistry*, 323(2), 731–740. <https://doi.org/10.1007/s10967-019-06973-0>
- Rahman, A. K. M. R., Meaze, A. K. M. M., Chakraborty, S. R., & Mohsin, M. (2019). Evaluations of n + <sup>27</sup>Al reaction in the energy range 0.1–200 MeV. *Indian Journal of Physics*, 94. <https://doi.org/10.1007/s12648-019-01555-y>
- Rahman, A. K. M. R., & Zubair, M. A. (2020a). Excitation functions of <sup>58</sup>Ni(n, charged particle) from threshold to 20 MeV using NLD models. *Indian Journal of Physics*, 95. <https://doi.org/10.1007/s12648-020-01808-1>
- Rahman, A. K. M. R., & Zubair, M. A. (2020b). Cross sections of <sup>56</sup>Fe(n, p)<sup>56</sup>Mn, <sup>55</sup>Mn(n, p)<sup>55</sup>Cr, <sup>52</sup>Cr(n, p)<sup>52</sup>V, <sup>56</sup>Fe(n, α)<sup>53</sup>Cr, <sup>55</sup>Mn(n, α)<sup>52</sup>V and <sup>52</sup>Cr(n, α)<sup>49</sup>Ti reactions using phenomenological level density models from threshold to 20 MeV. *Applied Radiation and Isotopes*, 166, 109429. <https://doi.org/https://doi.org/10.1016/j.apradiso.2020.109429>
- Reshid, T. S. (2013). Calculation of Excitation Function of Some Structural Fusion Material for (n, p) Reactions up to 25 MeV. *Journal of Fusion Energy*, 32(2), 164–170. <https://doi.org/10.1007/s10894-012-9541-5>
- Rohr, G., & Friedland, E. (1967). A study of neutron resonances of vanadium and manganese. *Nuclear Physics A*, 104(1), 1–16. [https://doi.org/10.1016/0375-9474\(67\)90753-1](https://doi.org/10.1016/0375-9474(67)90753-1)
- Shibata, K. (1989). Calculation of Neutron-Induced Reaction Cross Sections of Manganese-55. *Journal of Nuclear Science and Technology*, 26(10), 955–965. <https://doi.org/10.1080/18811248.1989.9734411>
- Takahashi, A., Sasaki, Y., Maekawa, F., & Sugimoto, H. (1989) Measurement and analysis of double differential neutron emission cross sections at En = 14.1 MeV for <sup>93</sup>Nb and <sup>181</sup>Ta (INDC(JPN)–118/L). International Atomic Energy Agency (IAEA).
- Thomson, D. B. (1963). Nuclear Level Densities and Reaction Mechanisms from Inelastic Neutron Scattering. *Physical Review*, 129(4), 1649–1667. <https://doi.org/10.1103/PhysRev.129.1649>
- Weigold, E. (1960). Cross Sections for the Interaction of 14-5 MeV Neutrons with Manganese and Cobalt. *Australian Journal of Physics*, 13(2), 186–188. <https://doi.org/10.1071/PH600186>
- Zamin, M. (1981). The Role of Mn in the Corrosion Behavior of Al-Mn Alloys. *Corrosion*, 37(11), 627–632. <https://doi.org/10.5006/1.3577549>